

ASIMINA TRILOBA SEEDS AS A FEEDSTOCK FOR ENERGY CONVERSION: OPTIMIZING YIELD RATE AND CHARACTERIZING FUEL PROPERTIES

Arunkumar SUBBIAH ^{1*}, Senthil Kumar BELLA RAMAN², Suresh VELLAIYAN³,
Prabha CHOCKALINGAM⁴

^{*1}Department of Mechatronics Engineering, Nehru Institute of Engineering and Technology,
Coimbatore, Tamilnadu, India

²Department of Aeronautical Engineering, Nehru Institute of Engineering and Technology,
Coimbatore, Tamilnadu, India

³Department of Sustainable Engineering, Saveetha School of Engineering, Saveetha Institute of
Medical and Technical Sciences, Chennai, Tamilnadu, India

⁴Department of Mechanical Engineering, Arjun College of Technology, Coimbatore, Tamilnadu, India

* Corresponding author; E-mail: drarunkumarsubbiah@gmail.com

In the present study, waste Asimina triloba seeds are proposed as a potential feedstock for biodiesel production, with the optimization of transesterification process parameters aimed at achieving higher yield rates. While previous studies have explored the use of Asimina triloba biodiesel for engine applications, this study stands out as the first to optimize transesterification process parameters for increased yield and to conduct comprehensive fuel characterization alongside storage stability analysis. The transesterification process parameters such as the methanol-oil molar ratio, catalyst volume concentration, reaction process temperature, and reaction process time are optimized by employing the response surface methodology. The response surface methodology analysis revealed that the proposed model is highly significant, with a coefficient of determination approaching unity. To achieve maximum biodiesel yield, the recommended parameters are a methanol-oil molar ratio of 14.7:1, a catalyst concentration of 2.4%, a reaction temperature of 81.3°C, and a reaction time of 138.8 minutes. Under these optimal conditions, the projected yield is 94.35%, aligning closely with experimental observations of 94.4%. The Fourier-transform infrared spectroscopy analysis underscored the substantial presence of carbon-based constituents in biodiesel, while the gas chromatography–mass spectrometry analysis revealed octadic-9,12-dienoic acid as the primary contributor. Furthermore, the stability profile demonstrates an extended stability period, complemented by physicochemical properties that align with the biodiesel standards specified by ASTM.

Key words: *Asimina triloba seeds; waste management; biodiesel; optimization; fuel characterization*

1. Introduction

In recent decades, the transportation sector has witnessed a substantial consolidation of petroleum products. However, the associated carbon dioxide emissions from the use of these petroleum-based products are major threats to the environment. Consequently, there is a growing realization that our dependence on petroleum resources is reaching its limits [1,2]. To address this challenge and reduce emissions from the transportation sector, it is imperative to adopt a new and sustainable perspective. Future transportation modes are expected to rely on a diverse range of energy sources, including electricity, hydrogen, and renewable biodiesel. An integrated approach to these energy alternatives holds the key to achieving environmental goals [3].

Biodiesel emerges as a promising strategy to curtail emissions in the transportation sector. It has demonstrated successful substitution for conventional diesel in a wide array of vehicles. Manufacturers worldwide are actively promoting biodiesel, with expectations of substantial production increases in the years ahead. Numerous studies have shown that transitioning to biodiesel could potentially reduce emissions by up to 90% over the engine's operational lifespan [4,5]. Biodiesel is a viable alternative to fossil fuels across various transportation modes and can blend with conventional fuels to enhance operational adaptability. This is particularly crucial in industries such as aviation, where even minor changes to existing systems require extensive safety assessments and could take years to implement [6]. Up to one thousand megatons of biodiesel could be produced sustainably around the world by 2040, thanks to the breadth of new unrefined components and technologies. This quantity would be sufficient to entirely replace the use of petroleum products in transportation [7].

Biodiesel is an important component of efforts to reduce emissions from transportation and promote more sustainable energy practices. Moreover, they have the advantage of being able to be blended with conventional fuels, facilitating seamless transitions and enhancing operational adaptability [8]. The use of first-generation biodiesels has a discernible impact on individuals' livelihoods within the food chain, but its influence on greenhouse gas emissions remains very negligible [9]. Second-generation fuels, derived from lignocellulosic biomass, are commonly referred to as biodiesel and are sourced from non-edible plant waste. Auxiliary factors, as opposed to fundamental factors, often exhibit a lesser degree of dependence on physical location. Generating second-generation biodiesel requires substantial investments and the development of novel technologies [10]. Third-generation biodiesels primarily utilize algae biomass, and fourth-generation biodiesels are powered by photobiological solar fuels [11].

Typically, a mechanical expeller is used to convert the vegetable or plant seed into bio-oil. Subsequently, the transesterification process is applied to create second-generation biodiesels [12]. Key factors influencing the transesterification process include the methanol-oil molar (MOM) ratio, catalyst volume concentration (CC), reaction process temperature (RTe), and reaction process time (RTm) [11]. Methanol, a fundamental constituent, undergoes ionization when subjected to a catalyst, leading to the decomposition of the strong base [12]. The reactor process temperature (RTe) plays a crucial role in transesterification, affecting the viscosity of the material and influencing diglyceride, monoglyceride, and methyl ester yields [13]. Given the sensitivity of biodiesel production costs to output rate and consumables, identifying the optimal process parameters becomes imperative.

In summary, exploring into the intricacies of second-generation biodiesels requires a comprehensive understanding of their feedstocks, transformation methods, and the critical parameters

influencing the transesterification process. The potential use of papaya fruit seeds, known as *Asimina triloba*, as a substrate for biodiesel production has been explored in this study. The investigation spans various sources of second-generation biodiesels, with the seeds of *Asimina triloba* emerging as an innovative substrate of interest. In India, papaya fruit production reached approximately 9.5 million kgs in 2022, with around 20% of the fruit's total fresh weight attributed to the seeds [14]. Despite their edibility, these seeds are commonly discarded as agricultural waste. The utilization of *Asimina triloba* biodiesel offers economic advantages by effectively tackling land use concerns while also diminishing greenhouse gas emissions. As the plants grow, they naturally sequester carbon dioxide, contributing to a reduction in overall greenhouse gas emissions. Moreover, the biodiesel exhibits lower carbon intensity compared to traditional diesel fuel, resulting in decreased net greenhouse gas emissions throughout its production and combustion processes [13,14]. The substantial lipid composition found in the seeds underscores their potential as a viable alternative to traditional oil sources. Diverse techniques have been employed for crude oil extraction from papaya seeds, with the prevalent constituent being the unsaturated fatty acid oleic acid.

While biodiesel production has been extensively studied, there is a notable dearth of research specifically focused on *Asimina triloba* seeds. Biodiesel production from these seeds can be achieved through transesterification, employing lipase as a catalyst, with a MOM ratio of 6:1 [15]. In a separate study, transesterification of crude *Asimina triloba* oil was accomplished using a two-stage catalytic approach with a MOM ratio of 9:1 [16]. Some investigations have explored synthesizing biodiesel from *Asimina triloba* seeds, utilizing copper oxide (CuO) and sodium hydroxide (NaOH) as catalysts. The transesterification process, conducted in a single stage with potassium hydroxide (KOH) as a catalyst, was also employed for biodiesel production from *Asimina triloba* [17, 18]. Methanol (CH₃OH), possessing strong basic properties and the potential for ionization with a catalyst, plays a crucial role in the transesterification process. The reactor process temperature (RTe) effectively aids in modifying material viscosity during transesterification. Vellaiyan [19] achieved a biodiesel production efficiency of 96.7% with a low volume concentration of sodium hydroxide catalyst and a MOM ratio of 9:1. Sivasubramanian [20] conducted biodiesel production through a one-step transesterification process, utilizing a sodium hydroxide catalyst and a methanol-to-oil molar ratio of 5:1. All the aforementioned sources unanimously affirm that papaya seed oil biodiesel exhibits essentially comparable physicochemical characteristics to conventional diesel fuel.

While numerous studies have delved into the natural regeneration and chemical composition of *Asimina triloba* seeds, none have specifically aimed to characterize *Asimina triloba* biodiesel (ATB) and assess its storage stability, nor have they attempted to refine the process parameters to optimize its production. Therefore, the primary objective of this research is to identify the optimal parameters for synthesizing biodiesel using the transesterification technique, with a specific focus on *Asimina triloba* seeds as the feedstock. To achieve the objectives, Response Surface Methodology (RSM) was employed, offering a robust optimization approach that considers multiple responses simultaneously. RSM stands out as a top choice for optimizing the transesterification process due to its effectiveness, adaptability, and ability to handle both linear and non-linear relationships between variables. Its statistical foundation allows for a comprehensive assessment of variables and their interactions, ensuring the reliability of biodiesel yield [7]. Bio-oil extraction from the seeds was accomplished using a mechanical expeller. The ATB yield rates were computed utilizing a Box-Behnken design matrix, enabling the systematic examination of various process parameters at different levels. To

validate the results, a confirmation experiment was conducted using the optimal process parameter settings. The functional groups of the produced ATB were analyzed through Fourier Transform Infrared (FTIR) spectroscopy, while the physicochemical parameters were assessed following the guidelines established by the ASTM. The chemical constituents present in the ATB was analyzed by gas chromatography–mass spectrometry (GC-MS), and storage stability of ATB was analyzed followed by accelerated oxidation test. These values were then compared with those of conventional biodiesel to evaluate its potential as a substitute for traditional diesel fuel.

2. Materials and methods

2.1 Preparation of *Asimina triloba* biodiesel

The *Asimina triloba* fruit seeds, integral to the production of ATB, were sourced from a local marketplace in close proximity. To enhance the quality of the seeds, a moisture reduction process was initiated, involving exposure to natural sunlight for approximately two days. The subsequent bio-oil extraction was carried out using a mechanical extraction method, resulting in a yield rate of 54.2% based on the dry weight of the sample. The transesterification process was executed using raw materials such as methanol (CH_3OH) and sodium phosphate (Na_3PO_4). A range of MOM ratios, spanning from 3:1 to 15:1, was achieved by employing varying volumes of bio-oil along with a reusable catalyst comprising 1% to 3% of the overall transesterification process. The experimental conditions covered a temperature range of 40 to 100 °C and a duration range of 60 to 150 minutes for the reactions. Post-transesterification, the resultant mixture of biodiesel, glycerine, and sodium phosphate underwent careful separation in a separating funnel. The methyl ester was extracted, leaving behind glycerine and sodium phosphate in the apparatus. Utilizing centrifugation effectively separated the residual catalyst from the mixture, enabling its subsequent reuse for three additional cycles. To eliminate impurities from the biodiesel, a water washing process was employed. The resulting biodiesel methanol blend was then utilized for characterizing and measuring its properties. This comprehensive process not only ensures the efficient production of *Asimina triloba* biodiesel but also highlights a sustainable approach through catalyst reuse and impurity elimination.

2.2 Methodology development using the Box-Behnken design matrix

The current optimization process focused on four key process parameters: MOM, CC, RTe, and RTm, all of which significantly impact the overall biodiesel yield rate. Transesterification, the conversion of fatty substances into methyl esters, requires the incorporation of methanol. However, an excess of methanol during the cycle can lead to suboptimal blending, resulting in the dilution of the catalyst [21]. Based on a prior optimization study, it was advised that a minimum MOM ratio of 3:1 be maintained during the transesterification of waste cooking oil. The investigation highlighted a negative correlation between the biodiesel yield rate and MOM ratio magnitude when it exceeds 15:1 [22]. Consequently, within the Box-Behnken design matrix, the MOM ratio's lower and upper limits were established as 3:1 and 15:1, respectively. The synthesis rate of unsaturated fat alkyl esters and glycerol can be elevated by employing a catalyst alongside an excess of methanol. The yield is influenced by a decrease in activation energy resulting from an increase in catalyst concentration [11]. A minimum catalyst concentration of 1% is deemed essential for successful transesterification execution. However, exceeding 3% catalyst concentration significantly affects overall biodiesel yield. Thus, the recommended range for CC was determined to be between 1% and 3%. Increasing RTe enhances

mixing rates, reducing the viscosity of the mixture. The low density of sodium phosphate leads to an increased scattering rate, accelerating the transformation process. Elevated temperatures during the transesterification process led to saponification [23]. Subsequent analysis determined the optimal temperature range for operations to be between 40 °C and 100 °C. The duration of residence in the reactor, denoted as RT_m , is critical for the complete conversion of fatty oils to methyl esters. A significant increase in RT_m enhances the probability of hydrolysis, potentially resulting in complete conversion into glycerine [22]. To transform oil into its corresponding methyl ester through the transesterification process, a minimum reaction time of 60 minutes is necessary. The biodiesel yield rate experiences a significant decrease beyond 150 minutes of heating duration. Consequently, the recommended time exposures for the process were determined to be between 60 minutes and 150 minutes.

2.3 Evaluation of fuel properties and characterization

The chemical composition of ATB was analyzed through FTIR spectra. This technique utilizes infrared radiation to identify specific atomic bonding frequencies, allowing for the identification of functional groups present in ATB. In the analysis of a particular functional group, infrared radiation exhibits distinct peaks at varying wavelengths. The chemical bonds were determined based on the peaks and wavenumbers within the infrared spectrum, which typically ranges from 400 cm^{-1} to 4000 cm^{-1} . GC-MS analysis stands out as the preferred method for quantifying long and branched-chain hydrocarbons, volatile matter, esters, and alcohols. Within this methodology, the ATB sample is introduced into the system, where the temperature is gradually raised to a maximum of 300 degrees Celsius. During this process, a surface material efficiently extracts the various chemicals generated from the sample. These extracted compounds are then subjected to analysis using a mass spectrometer. This approach enables precise identification and quantification of each individual constituent present in the sample, ensuring accurate characterization of its composition. The storage stability of the samples was assessed using the accelerated oxidation test method outlined in EN 14112. The process involved subjecting the ester samples to oxidation at 120 °C, while a continuous airflow of 10 liters per hour passed over them. The formation of volatile acids signaled the conclusion of the induction period (IP), identified by a rapid increase in conductivity. Physicochemical properties of the sample were assessed by measuring density and viscosity using a hydrometer and a capillary viscometer, respectively, at temperatures of 15 and 40 °C. These reference temperatures align with ASTM D1298 and ASTM D445 standards, respectively. The calorific value (CV) of ATB was determined using a bomb calorimeter, following the specifications outlined in ASTM D240. Furthermore, the flash point (FP) of ATB was determined using a closed-cup flash point device, as per ASTM D93 standards. The copper strip corrosion (CSC) test, in accordance with ASTM standard D1838, was conducted under controlled conditions for three hours at a temperature of 50 °C. To determine the cloud point and pour point of ATB, tests were performed following ASTM D97 and ASTM D2500 standards, respectively.

3. Results and discussion

3.1. Yield rate as a function of process parameters

Tab. 1 presents the Box-Behnken design matrix, providing a comprehensive overview of experimental and expected yield rates corresponding to different levels of process parameters. The experimental results indicate that, despite high values for RT_e and RT_m , the yield rate decreases due

to the constraint imposed by the minimum concentrations of MOM ratio and CC. Notably, a higher MOM ratio magnitude consistently leads to increased ATB yield across all experimental trials. The design matrix reflects a diverse range of yield rates, spanning from 54.7% in Run No. 25 to 91.6% in Run No. 13. It is evident that the combinations of MOM ratio and CC process parameters play a significant role in influencing the overall performance of the biodiesel production process. Additionally, it is observed that RTe exerts a relatively minor influence on ATB yield. Specifically, when RTe is low and the MOM ratio is medium, the occurrence of immiscibility hampers optimal methyl ester conversion. These findings underscore the intricate interplay between key parameters, emphasizing the importance of balancing MOM ratio, CC, and RTe for maximizing ATB yield in the transesterification process.

Table 1. Optimization using Box-Behnken design

Run No	MOM Ratio	CC (%)	RTe (deg C)	RTm (min)	ATB yield	
					Actual	Predicted
1	3	2	100	105	70.6	70.46
2	9	2	100	60	62.9	62.99
3	9	1	70	150	74.2	73.98
4	15	3	70	105	84.4	84.71
5	9	2	40	60	56.9	56.78
6	15	2	70	60	62.8	62.55
7	15	1	70	105	76.6	76.66
8	9	2	70	105	91.1	91.44
9	3	1	70	105	59.7	59.48
10	9	3	100	105	80.6	80.5
11	3	3	70	105	73	73.03
12	9	2	70	105	91.5	91.44
13	9	2	70	105	91.6	91.44
14	9	3	70	60	63.1	63.31
15	3	2	40	105	63.4	63.64
16	15	2	70	150	91.4	91.42
17	9	1	100	105	75.3	75.5
18	9	2	70	105	91.5	91.44
19	9	3	70	150	87.3	87.13
20	9	1	40	105	62.3	62.33
21	9	3	40	105	79.2	78.93
22	15	2	40	105	77.4	77.53
23	15	2	100	105	85.7	85.44
24	9	2	70	105	91.5	91.44
25	9	1	70	60	54.7	54.86
26	3	2	70	150	69.4	69.58
27	3	2	70	60	55.6	55.52
28	9	2	100	150	85.4	85.61
29	9	2	40	150	77.1	77.09

3.2. Analysis of variance

Tab. 2 presents the analysis of variance (ANOVA) findings for the quadratic model, offering insights into the impact of different variables on ATB yield. The mean square values reveal that the MOM ratio variable exerts a substantial impact of 24.8% on ATB yield. In contrast, the CC variable demonstrates a relatively lower impact at 13.9%, while the RTe variable exhibits the least impact at 6.5%. Remarkably, the RTm variable emerges as the most influential, with a significant impact of 54.8% on ATB yield. RTe has a comparatively lesser effect on ATB yield than the other three parameters. To assess the model's validity, the probability of error is estimated at 0.01%, contingent on the F-value exceeding 4724.88 and the P-value being below 0.0001. The F-value of 1.98 suggests that any discrepancies observed are not significantly substantial in relation to the overall error. Furthermore, the model is robustly supported by its statistically significant p-value (<0.0001) and a substantial lack of fit (>0.05). To predict the outcome of a reaction involving specific quantities of each element, an equation incorporating significant variables is employed. The equation is formulated to represent ATB yield as a dependent variable influenced by several significant factors as follows:

$$ATB\ yield = -128.45 + 4.62111 * A + 47.3342 * B + 1.52723 * C + 1.34621 * D - 0.229167 * AB + 0.00152778 * AC + 0.0137037 * AD - 0.0966667 * BC + 0.0261111 * BD + 0.000425926 * CD - 0.250324 * A^2 - 8.96167 * B^2 - 0.00906852 * C^2 - 0.00625267 * D^2 \quad (1)$$

where 'A' represents the MOM ratio, 'B' represents the volume concentration of CC, 'C' represents the RTe, and 'D' represents the 'RTm'.

The statistical significance observed in ANOVA indicates that every factor and interaction incorporated into the model plays a significant role in elucidating the variance observed in the response variable. This suggests that all factors and interactions examined in the research exert a statistically significant impact on the biodiesel yield under investigation.

Table 2. ANOVA

Source	Sum of Squares	df	Mean Square	F-value	p-value
Model	4277.59	14	305.54	4724.88	< 0.0001
A-MOM	624.96	1	624.96	9664.38	< 0.0001
B-CC	349.92	1	349.92	5411.13	< 0.0001
C-RTe	162.8	1	162.8	2517.58	< 0.0001
D-RTm	1382.45	1	1382.45	21378.1	< 0.0001
AB	7.56	1	7.56	116.95	< 0.0001
AC	0.3025	1	0.3025	4.68	0.0483
AD	54.76	1	54.76	846.8	< 0.0001
BC	33.64	1	33.64	520.21	< 0.0001
BD	5.52	1	5.52	85.4	< 0.0001
CD	1.32	1	1.32	20.45	0.0005
A ²	526.77	1	526.77	8145.9	< 0.0001

B ²	520.94	1	520.94	8055.76	< 0.0001
C ²	432.08	1	432.08	6681.7	< 0.0001
D ²	1039.9	1	1039.9	16080.9	< 0.0001
Lack of Fit	0.7533	10	0.0753	1.98	0.2662
< 0.0001: significant; >0.05: not significant					

3.3. Impact of key variables on *Asimina triloba* biodiesel yield

Fig. 1 represents the impact of process parameter variations on the ATB yield. Fig. 1(a) illustrates the changes in ATB yield with respect to variations in MOM and CC levels, while keeping RTe and RTm values constant. This figure reveals a positive correlation between a higher MOM ratio and an increased ATB yield, emphasizing the importance of augmenting the MOM ratio to enhance ATB yield. An increased concentration of methanol beyond the stoichiometric requirement is shown to accelerate mass transfer rates and achieve an equilibrium state [24], aligning with evidence from the ANOVA table indicating MOM ratio's impact on ATB yield. Higher MOM ratios enhance the catalyst's efficiency. The figure also highlights a decrease in ATB yield under elevated reaction temperatures, primarily attributed to an immiscibility issue arising from increased MOM ratio and CC. Using the median as a measure of central tendency for MOM ratio and CC, there is an observed around 12% decrease in ATB yield. Fig. 1(b) estimates variations in ATB yield concerning variations in MOM ratio and RTe levels while keeping CC and RTm constant. The decrease in ATB yield is attributed to higher temperatures leading to methanol evaporation, consistent with prior research [25]. The variations in ATB yield based on MOM ratio and RTm are illustrated in Fig. 1(c), with both CC and RTe held constant. Higher yield of ATB is achieved by augmenting the other two process parameters along with elevations in MOM and slight extensions in reactor residence time. However, it's essential to note that an increase in reaction temperature may lead to a decrease in yield rates due to potential reactant hydrolysis.

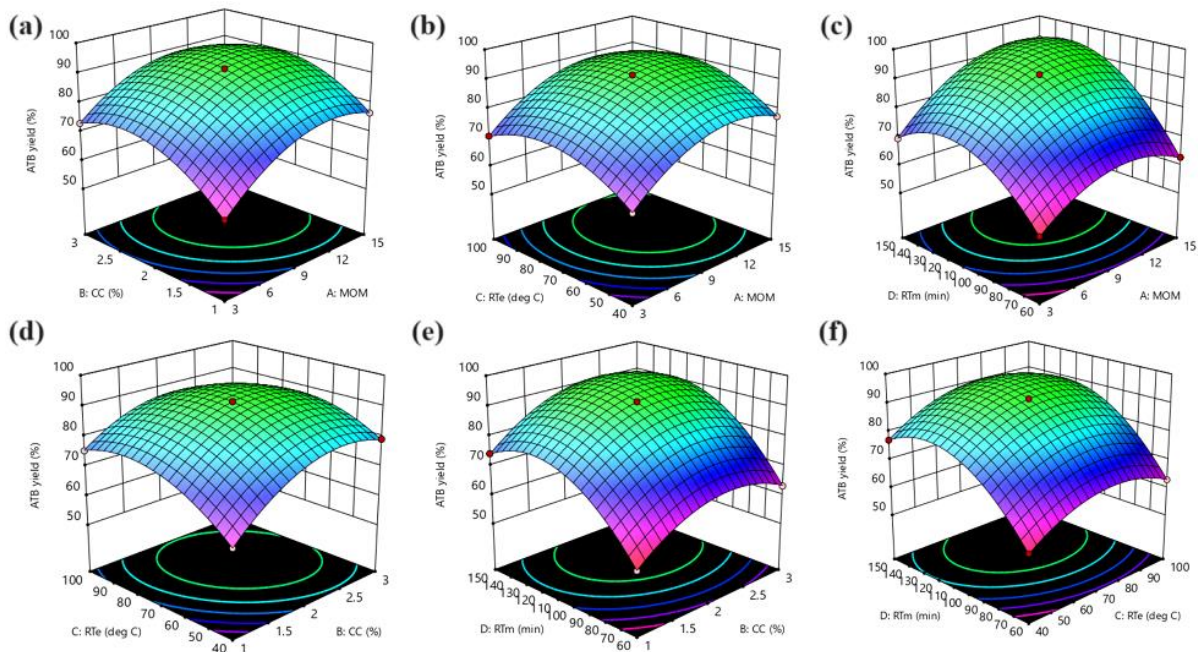


Figure 1. Impact of process parameters on ATB yield

Figs. 1(d) and 1(e) illustrate the combined impact of CC, RTe, and RTm on the yield of ATB. The influence of RTe on ATB yield is observed to be minimal, consistent with evidence from the ANOVA table. Both figures provide evidence supporting the data that an increase in CC, up to approximately 3%, has a favorable effect on ATB yield. However, surpassing this threshold results in a decline in ATB yield. The presence of a catalyst reduces the activation energy required for transesterification, leading to an accelerated reaction rate. Beyond a 2% increase in CC, there is a gradual decline in ATB yield. The high viscosity of sodium phosphate, when an excessive amount of catalyst is added, contributes to increased viscosity and decreased mixing and mass transfer rates, ultimately reducing ATB yield [24]. Additionally, it's noteworthy that glycerine exhibits a significant degree of conversion for CC compounds. Figure 1(d) illustrates estimated variations in ATB yield resulting from changes in CC and RTe, with the MOM ratio and RTm held constant. Fig. 1(e) provides an estimation of ATB yield resulting from variations in CC and RTm, with the MOM ratio and RTe values held constant. These visualizations offer valuable insights into the interdependencies of CC, RTe, and RTm, providing a basis for optimizing their values to maximize ATB yield in the transesterification process.

Fig. 1(f) illustrates the impact of RTm on the yield of the ATB in relation to RTe, with the constant utilization of MOM ratio and CC. The data presented in the figure supports and aligns with the earlier discussed findings that indicated RTe did not exert a significant impact on ATB yield. The investigation acknowledges that achieving complete conversion of triglyceride into methyl ester requires an adequate reaction time due to the three distinct phases involved in the transesterification process [26]. The graph illustrates a positive correlation between the increase in RTm and an equivalent rise in ATB yield. However, a substantial increase in ATB yield is only observed when RTm reaches approximately 140 minutes. It is emphasized that exceeding a specific threshold in RTm may lead to hydrolysis, diminishing the yield and increasing the probability of glycerine conversion instead of methyl ester formation. Gurusamy et al. [3] also reported that a higher RTm during the transesterification process increases the likelihood of reactions between impurities and triglycerides, which could lead to hydrolysis.

3.4. Confirmation test and process parameters at their optimal levels

The optimization procedure involved assigning different ranges to significant process parameters. To enhance the yield of ATB, the output response was assessed under the 'maximum-the-best' condition. The optimal values for the process parameters are as follows: MOM ratio = 14.7:1, CC = 2.4%, RTe = 81.3 °C, and RTm = 138.8 minutes. Under these conditions, the projected yield for ATB is 94.35%. Fig. 2 represents the optimal value of process parameters and the ATB yield (projected value) at optimum condition. To validate the projected ATB yield, experimental validation was conducted, maintaining the identified optimal conditions. The experimental investigation confirmed that the ATB yield attained an average value of 94.4% over five distinct experiments, with a relative standard deviation below 0.2%, indicating a high level of accuracy in the experimental results.

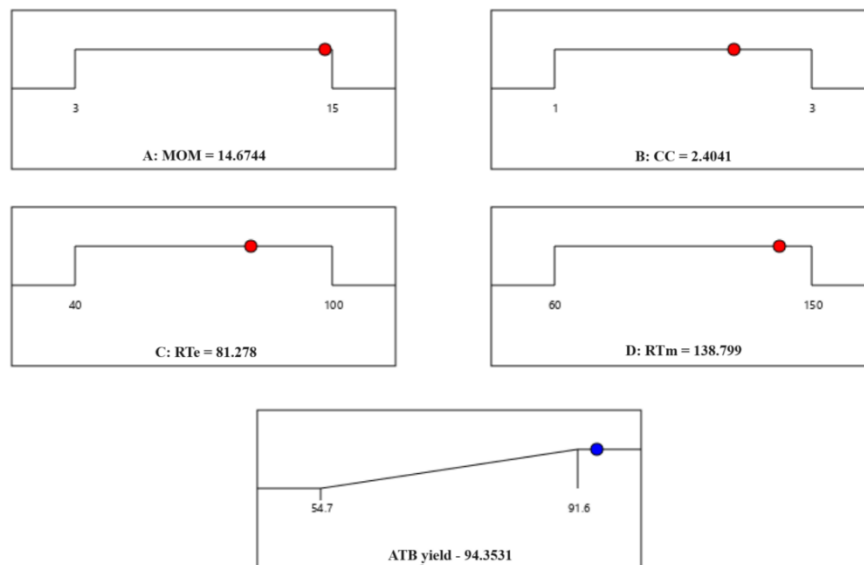


Figure 2. Optimum level and corresponding yield

3.5. Fuel characterization and storage stability

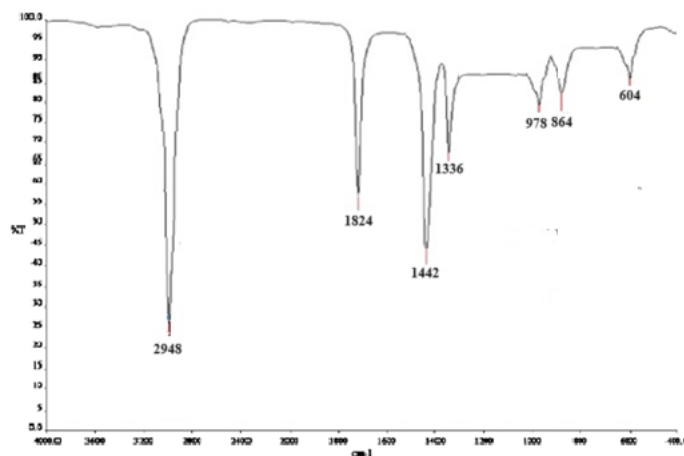


Figure 3. FTIR spectra of ATB

Various functional groups present in the ATB were identified using FTIR analysis, and Fig. 3 illustrates the FTIR spectra of ATB. Infrared radiation tends to undergo chemical reactions upon interaction with specific chemical species, and the identification of functional groups is achieved through the analysis of the detected absorption spectra. The FTIR research findings reveal distinctive features in the ATB spectrum. Saturated hydrocarbons exhibit a characteristic C-H stretching vibration at a wavelength of 2945 cm^{-1} , while the C=C stretching functional groups of alkenes are evident at a wavenumber of 1824 cm^{-1} . The presence of absorption at 1442 cm^{-1} suggests the existence of a carbon-hydrogen (CH) bond, and the C-O bond is observed at 1336 cm^{-1} . Additionally, wavenumbers at 978 cm^{-1} indicate the presence of a second alkene functional group, specifically a carbon-oxygen-hydrogen (C-OH) bond. The FTIR analysis of the ATB reveals significant peaks related to ester groups, which result from the presence of fatty acid methyl esters. In contrast, diesel fuel comprises alkanes, cycloalkanes, and aromatic compounds. The ester groups present in the ATB can effectively

complement the functions of hydrocarbon groups, making it a promising alternative to traditional diesel fuel. This is substantiated by the significant contributions of carbon, hydrogen, and oxygen bonds observed in the overall evaluation of ATB, as evidenced by the FTIR results [26].

Figure 4 presents the results of the GC-MS analysis performed on the synthesized ATB. Notably, the absence of a saponification process precluded the characterization of raw oil in this study. Upon examination, it is evident that linoleic acid comprises the predominant component, constituting about 60% of the total fatty acids in the synthesized ATB. Hexadecanoic and octadecanoic acids contribute about 20% and 17%, respectively. The collective contribution of other fatty acids throughout the composition accounts for about 3%.

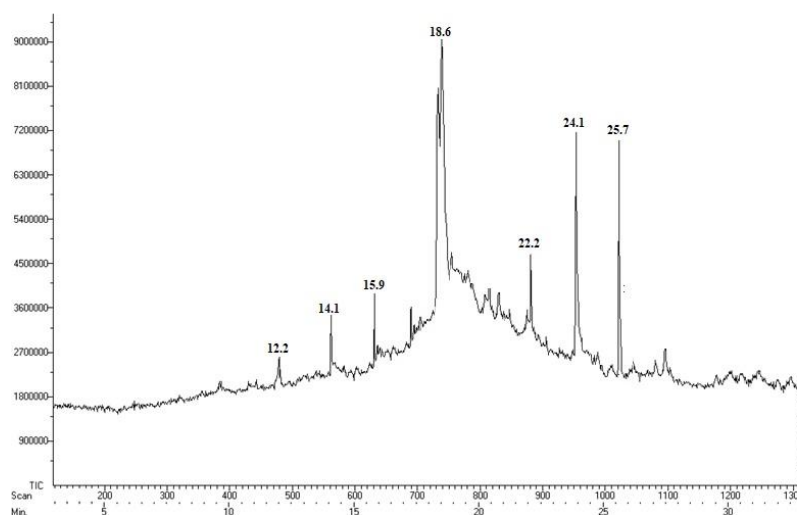


Figure 4. GC-MS analysis of ATB

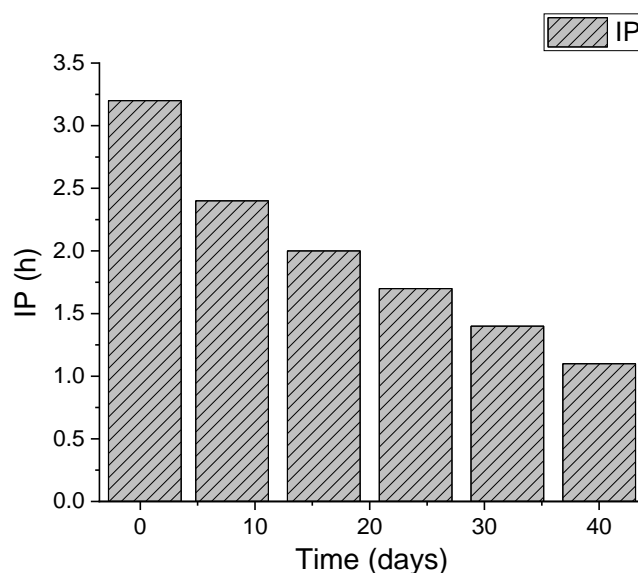


Figure 5. Dependence of IP upon storage time

An investigation into the oxidation stability of ATB over extended storage durations was undertaken, focusing on the induction period (IP). As depicted in Figure 5, initially, the IP surpassed three hours at 0.4 days. However, by the eighth day, it notably diminished to 2.4 hours, signifying a substantial reduction. Continuing the storage led to a gradual decline in the IP, with the onset of

autooxidation becoming apparent. Nevertheless, even after forty days had passed, the IP remained above one hour.

The examination of the physicochemical properties of the proposed ATB revealed that all essential characteristics conform to the permissible limits as defined by the ASTM 6751 standard. Tab. 3 provides a comparative analysis of the physical and chemical attributes of the proposed ATB and conventional diesel fuels. ATB fuel exhibits a higher density and viscosity compared to diesel, with increases of 3.7% and 41.3%, respectively. Despite these variations, the corrosion test results indicate that ATB demonstrated a class 1a classification, equivalent to that of conventional diesel fuel. It is noteworthy that the calorific value of ATB was found to be 5.8% lower than that of diesel fuel. However, ATB presents a significantly higher flash point compared to diesel fuel, ensuring enhanced safety during handling and storage [27-29]. The assurance of ATB's compatibility at low working temperatures is derived from its cloud point and pour point, both of which align with the prescribed limits outlined in the relevant ASTM standard. This comprehensive analysis underscores the overall compliance of ATB with industry standards and highlights its potential as a viable and safe alternative to conventional diesel fuel.

Table 3. Physicochemical properties of BMB and its comparison with normal diesel fuel

Properties	Diesel	ATB	ASTM limits	method
Density @ 15 °C (kg/m ³)	829.3	860.4	860-900	ASTMD4052
Viscosity @ 40 °C (mm ² /sec)	2.9	4.1	1.9 – 6.0	ASTMD445
Calorific value (kJ/kg)	42900	40400	NA	ASTMD240
Copper strip corrosion @ 50 °C, for 3h	1a	1a	Max 3	ASTMD1838
Flash point (°C)	61	10	min 130°C	ASTMD93
Cloud point (°C)	2	5	-3 to 12	ASTMD97
Pour point (°C)	1	4	-15 to 20	ASTMD2500

4. Conclusion

The primary aim of this study is to optimize the transesterification process parameters for obtaining higher biodiesel yield from *Asimina triloba* seeds waste. The Box-Behnken design matrix was employed to systematically evaluate the impact of various process parameters on ATB yield, Fuel samples underwent thorough characterization using FTIR, GC-MS, storage stability, and physicochemical properties analysis. The experiments revealed that the optimal transesterification parameters for maximizing ATB yield are a MOM ratio of 14.7:1, CC of 2.4%, RTe of 81.3 °C, and RTm of 138.8 minutes. The coefficient of determination for the ATB yield approached unity, signifying a robust correlation among the variables. Under optimal conditions, the projected ATB yield is 93.53%, while experimental outcomes demonstrate a yield of 94.4%. The negligible disparity of less than 0.2% between theoretical and actual findings underscores the model's accuracy. FTIR analysis highlighted the significance of hydrocarbon and alkene functional groups in the proposed

ATB. The GC-MS analysis showed that octadic-9,12-dienoic acid makes up approximately 60% of the composition, while the stability profile indicates that ATB maintains its stability for over 40 days during storage. Physicochemical measurements indicate ATB's compatibility with conventional diesel fuel, meeting biodiesel requirements outlined by ASTM standards. Potential directions for future research may involve conducting a comprehensive combustion performance and emission analysis. Additionally, performing vibration analysis could complement the evaluation of ATB as a promising alternative to conventional fuel for real-time implementation.

References

- [1] Harikrishnan,A., et al., Performance, emission characteristics of CI engines fueled with Annona seed biodiesel blends and 1-pentanol as an additive, *Thermal Science*, 27 (2023), 4(A), pp.2957–2965. <https://doi.org/10.2298/tsci221126090a>.
- [2] Soudagar,M.E.M., et al., Effect of Sr@ ZnO nanoparticles and Ricinus communis biodiesel-diesel fuel blends on modified CRDI diesel engine characteristics, *Energy*, 215 (2021), p.119094. <https://doi.org/10.1016/j.energy.2020.119094>
- [3] Gurusamy,M., et al., Optimization of process parameters to intensify the yield rate of biodiesel derived from waste and inedible Carthamus lanatus (L.) Boiss. seeds and examine the fuel properties with pre-heated water emulsion, *Sustainable Chemistry and Pharmacy*, 33 (2023), p.101137. <https://doi.org/10.1016/j.scp.2023.101137>
- [4] Krishnan,M.G., et al., Exploring the synergistic potential of higher alcohols and biodiesel in blended and dual fuel combustion modes in diesel engines: A comprehensive review, *Sustainable Chemistry and Pharmacy*, 35 (2023), p.101180. <https://doi.org/10.1016/j.scp.2023.101180>
- [5] Ahmad,A., et al., A hybrid RSM-GA-PSO approach on optimization of process intensification of linseed biodiesel synthesis using an ultrasonic reactor: Enhancing biodiesel properties and engine characteristics with ternary fuel blends, *Energy*, 288 (2024), p.129077. <https://doi.org/10.1016/j.energy.2023.129077>
- [6] Bibin,C., et al., Environment impact assessment of agricultural diesel engines utilizing biodiesel derived from phoenix sylvestris oil, *Environmental Research*, 224 (2023), p.115432. <https://doi.org/10.1016/j.envres.2023.115432>
- [7] Samuel,O.D., et al., Modelling of Nicotiana Tabacum L. oil biodiesel production: comparison of ANN and ANFIS, *Frontiers in Energy Research*, 8 (2021), p.612165. <https://doi.org/10.3389/fenrg.2020.612165>
- [8] Thippeshnaik,G., et al., Experimental investigation of compression ignition engine combustion, performance, and emission characteristics of ternary blends with higher alcohols (1-Heptanol and n-Octanol), *Energies*, 16 (2023), p.6582. <https://doi.org/10.3390/en16186582>
- [9] Soudagar,M.E.M., et al., The effects of graphene oxide nanoparticle additive stably dispersed in dairy scum oil biodiesel-diesel fuel blend on CI engine: performance, emission and combustion characteristics, *Fuel*, 257 (2019), p.116015. <https://doi.org/10.1016/j.fuel.2019.116015>

- [10] Venkatesan,H., et al., Optimized biodiesel production from *C. innophyllum* bio-oil using Kriging and Ann predictive models, *Thermal Science*, 26 (2022), 5(B), pp.4217–4232. <https://doi.org/10.2298/tsci211127032v>
- [11] Ahmad,A., et al., Predictive Modeling and Optimization of Engine Characteristics with Biogas–Biodiesel-Powered Dual-Fuel Mode: A Neural Network-Coupled Box–Behnken Design, *Arabian Journal for Science and Engineering*, 49 (2024), pp.2661-2680. <https://doi.org/10.1007/s13369-023-08375-7>
- [12] Zhu,Z., et al., Soybean biodiesel production using synergistic CaO/Ag nano catalyst: Process optimization, kinetic study, and economic evaluation, *Industrial Crops and Products*, 166 (2021), p.113479. <https://doi.org/10.1016/j.indcrop.2021.113479>
- [13] Soudagar,M.E.M., et al., Investigation on the effect of cottonseed oil blended with different percentages of octanol and suspended MWCNT nanoparticles on diesel engine characteristics, *Journal of Thermal Analysis and Calorimetry*, 147 (2022), pp.525-542. <https://doi.org/10.1007/s10973-020-10293-x>
- [14] Soudagar,M.E.M., et al., Study of diesel engine characteristics by adding nanosized zinc oxide and diethyl ether additives in Mahua biodiesel–diesel fuel blend, *Scientific reports*, 10 (2020), p.15326. <https://doi.org/10.1038/s41598-020-72150-z>
- [15] Ahmad,A., et al., Enhancing waste cooking oil biodiesel yield and characteristics through machine learning, response surface methodology, and genetic algorithms for optimal utilization in CI engines, *International Journal of Green Energy*, 21 (2024), pp.1345-1365. <https://doi.org/10.1080/15435075.2023.2253870>.
- [16] Ngige,G.A., et al., RSM optimization and yield prediction for biodiesel produced from alkali-catalytic transesterification of pawpaw seed extract: Thermodynamics, kinetics, and Multiple Linear Regression analysis, *Digital Chemical Engineering*, 6 (2023), p.100066. <https://doi.org/10.1016/j.dche.2022.100066>
- [17] Anwar,M., et al., A Systematic Multivariate Analysis of Carica papaya Biodiesel Blends and Their Interactive Effect on Performance, *Energies*, 11 (2018), p.2931. <https://doi.org/10.3390/en11112931>
- [18] Daryono,E.D., Rapid In Situ Transesterification of Papaya Seeds to Biodiesel with The Aid of Co-solvent, *International Journal of Renewable Energy Research*, 7 (2017), pp.379-385. <https://doi.org/10.20508/ijrer.v7i1.5275.g6998>
- [19] Vellaiyan,S., Energy conversion from *Bauhinia malabarica* seed as novel feedstock—optimisation for higher yield rate and fuel characterization, *Biomass Conversion and Biorefinery*, 2023, pp.1-14. <https://doi.org/10.1007/s13399-023-03989-1>
- [20] Sivasubramanian,H., Performance and emission characteristics of papaya seed oil methyl ester–n-butanol–diesel blends on a stationary direct-injection CI engine, *Biofuels*, 9 (2018), 4, pp. 513-522. <https://doi.org/10.1080/17597269.2017.1291878>
- [21] Samuel,O.D., et al., Comparison of the techno-economic and environmental assessment of hydrodynamic cavitation and mechanical stirring reactors for the production of sustainable hevea

Brasiliensis ethyl ester, *Sustainability*, 15 (2023), 23, p.16287.

<https://doi.org/10.3390/su152316287>

- [22] Ahmad,A., et al., Application of machine learning and genetic algorithms to the prediction and optimization of biodiesel yield from waste cooking oil, *Korean Journal of Chemical Engineering*, 40 (2023), 12, pp.2941-2956. <https://doi.org/10.1007/s11814-023-1489-9>
- [23] Samuel,O.D., et al., Production of fatty acid ethyl esters from rubber seed oil in hydrodynamic cavitation reactor: Study of reaction parameters and some fuel properties, *Industrial Crops and Products*, 141 (2019), p.111658. <https://doi.org/10.1016/j.indcrop.2019.111658>
- [24] Soudagar,M.E.M., et al., An investigation on the influence of aluminium oxide nano-additive and honge oil methyl ester on engine performance, combustion and emission characteristics, *Renewable Energy*, 146 (2020), pp.2291-2307. <https://doi.org/10.1016/j.renene.2019.08.025>
- [25] de S.Barros,S., et al., Pineapple (Ananás comosus) leaves ash as a solid base catalyst for biodiesel synthesis, *Bioresource Technology*, 312 (2020), 123569. <https://doi.org/10.1016/j.biortech.2020.123569>
- [26] Effiom,S.O., et al., Cost, Emission, and Thermo-Physical Determination of Heterogeneous Biodiesel from Palm Kernel Shell Oil: Optimization of Tropical Egg Shell Catalyst, *Indonesian Journal of Science and Technology*, 9 (2024), pp.1-32. <https://doi.org/10.17509/ijost.v9i1.64006>
- [27] Elkelawy,M., et al., Maximization of biodiesel production from sunflower and soybean oils and prediction of diesel engine performance and emission characteristics through response surface methodology, *Fuel*, 266 (2020), p.117072. <https://doi.org/10.1016/j.fuel.2020.117072>.
- [28] Samuel,O.D., et al., Prandtl number of optimum biodiesel from food industrial waste oil and diesel fuel blend for diesel engine, *Fuel*, 285 (2021), p.119049. <https://doi.org/10.1016/j.fuel.2020.119049>.
- [29] Ahmad,A., et al., Process optimization of spirulina microalgae biodiesel synthesis using RSM coupled GA technique: a performance study of a biogas-powered dual-fuel engine, *International Journal of Environmental Science and Technology*, 21, (2024), pp.168-188. <https://doi.org/10.1007/s13762-023-04948-z>

RECEIVED DATE: 21.10.2023

DATE OF CORRECTED PAPER: 16.12.2023

DATE OF ACCEPTED PAPER: 28.3.2024.